# Highlights from the LHCb ion physics program

**Michael Schmelling** on behalf of the LHCb collaboration

Max Planck Institute for Nuclear Physics, Saupfercheckweg 1, 69117 Heidelberg, Germany

E-mail: `Michael.Schmelling@mpi-hd.mpg.de`

**Abstract.**  Following the successful participation of LHCb in the 2013 proton-lead run of the LHC, in 2015 the collaboration decided to further extend its physics program to study also lead-lead collisions and fixed target interactions. These proceedings discuss the physics reach of the detector and the first results from the LHCb ion physics and fixed target program.

## 1. Introduction

Although the QCD Lagrangian is well understood, phenomenological models still dominate the description of strong interactions at small momentum transfers or in the regime of high pressure and density, *i.e.* generally in processes that cannot be handled in perturbation theory. At high energy density a so-called quark-gluon plasma (QGP) is expected to form. Properties of the QGP can *e.g.* be probed by heavy flavour particles [1], where heavy quarks are produced in hard parton-parton interactions and then evolve in the strongly interacting medium. Comparing the particle production properties in central Pb-Pb collisions, where a QGP is expected to form, with those in $p$-Pb collisions, allows to disentangle genuine QGP signatures from effects of the cold nuclear medium. Those so-called cold nuclear matter effects, such as modifications of the parton densities inside the bound nucleons [2] or energy-loss of heavy particles in the medium [3], can be studied by comparing production characteristics in $pp$ and $p$-Pb collisions.

## 2. LHCb detector and physics reach

The LHCb detector [4, 5] is a single-arm forward spectrometer covering the pseudorapidity range $2 < \eta < 5$, designed for the study of particles containing $b$ or $c$ quarks. The detector includes a high-precision tracking system consisting of a silicon-strip vertex detector surrounding the $pp$ interaction region, a large-area silicon-strip detector located upstream of a dipole magnet with a bending power of about $4\,\mathrm{Tm}$, and three stations of silicon-strip detectors and straw drift tubes placed downstream of the magnet. The tracking system provides a measurement of momentum, $p$, of charged particles with a relative uncertainty that varies from 0.5% at low momentum to 1.0% at $200\,\mathrm{GeV}/c$. The minimum distance of a track to a primary vertex, the impact parameter, is measured with a resolution of $(15 + 29/p_\mathrm{T})\,\mathrm{\mu m}$, where $p_\mathrm{T}$ is the component of the momentum transverse to the beam, in $\mathrm{GeV}/c$. Different types of charged hadrons are distinguished using information from two ring-imaging Cherenkov detectors. Photons, electrons and hadrons are identified by a calorimeter system consisting of scintillating-pad and preshower detectors, an electromagnetic calorimeter and a hadronic calorimeter. Muons are identified by a system composed of alternating layers of iron and multiwire proportional chambers. The online event selection is performed by a trigger, which consists of a hardware stage,
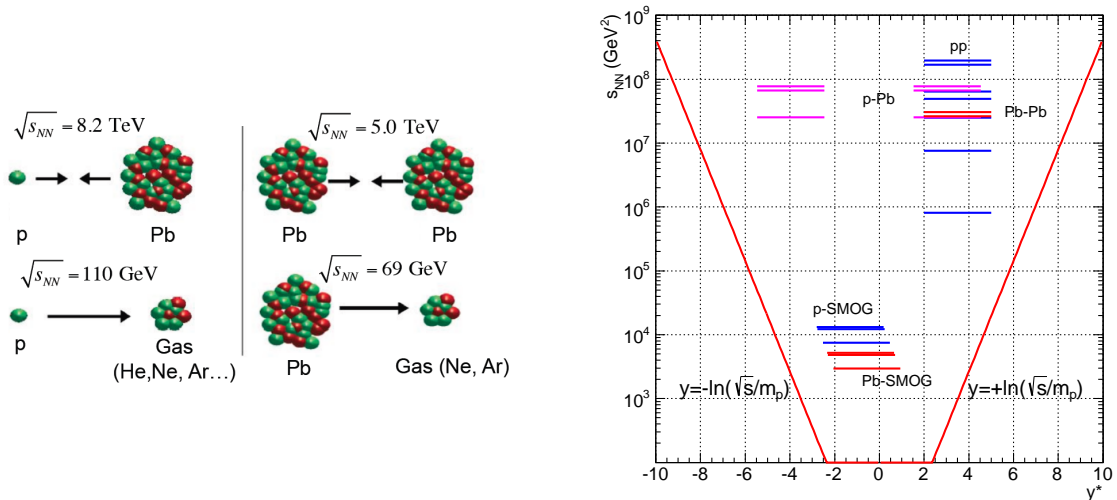
**Figure 1.** Ion physics running modes and kinematic coverage of LHCb

based on information from the calorimeter and muon systems, followed by a software stage, which applies a full event reconstruction.

Figure 1 (left) shows the heavy-ion operation modes of the LHCb experiment. With colliding beams, $p$-Pb and Pb-Pb collisions can be studied at nucleon-nucleon centre-of-mass energies in the multi-TeV regime. In addition, the LHCb SMOG system (*System for Measuring Overlap with Gas*) [6] allows to inject small amounts of gas into the beam vacuum. Initially designed for luminosity determination based on beam-profile measurements by means of beam-gas interactions [7], the SMOG system enables in addition the study of fixed target interactions with $p$-A and Pb-A collision at nucleon-nucleon centre-of-mass energies of $O(10^2)$ GeV. The possibility of doing fixed target physics was first demonstrated by recording $p$-Ne collisions in parallell to a test of the SMOG system during in the 2012 $p$-Pb pilot run [8], showing that LHCb is able to span the physics from SPS and RHIC energies to the LHC in a single experiment. The phase space where particle production measurements can be performed is sketched in Fig. 1 (right). For symmetric configurations the detector has forward coverage between 2 and 5 units in rapidity for all centre-of-mass energies. In fixed target mode, with the forward direction defined by the beam particle, the coverage is central to slightly backward, depending on the beam energy and type of projectile. For $p$-Pb collisions, depending on the orientations of the beams, both the forward and the backward hemisphere can be probed.

## 3. Proton-lead collisions

Analyses of $p$-Pb collisions performed to date by the LHCb collaboration cover quarkonium production [9–11], $Z$-boson production [12], $D^0$ production [13] and the study of long-range near-side correlations in high multiplicity events [14].

Because of space limitations, the following focuses on charm production measurements in $p$-Pb collisions, where $J/\psi$ and $\psi(2S)$ mesons are reconstructed via decays into two muon final states. Here the excellent performance of the LHCb vertex detector allows to disentangle prompt from secondary production via $b$ meson decays by means of the so-called pseudo proper-time $t_z = L_z m/p_z$, where $L_z$ is the distance between primary vertex and secondary vertex along the beam direction $z$, $p_z$ is the momentum component of the charmonium candidate along $z$ and $m$ the known mass of the charmonium state. Figure 2 illustrates how prompt and delayed components are disentangled [9]. Signal and background are separated by means of the invariant mass. The *sPlot* technique [19] is used to determine the lifetime distribution of the background, which is then fixed in the fit to the $t_z$ distribution that determines the prompt and delayed components.
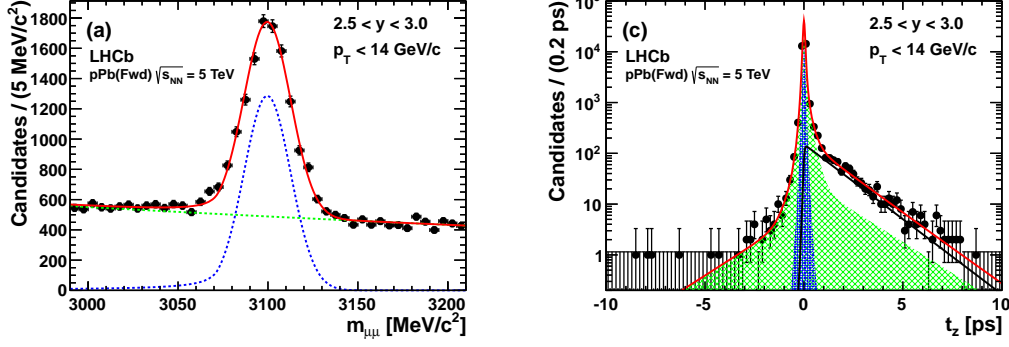
**Figure 2.** Example from the study of $p$-Pb collisions [9] for the use of (left) invariant mass and (right) pseudo proper-time to disentangle prompt and delayed production of charmonium states.

Variables which allow to quantify nuclear effects, such as modifications of the parton densities of the bound nucleons (shadowing) or energy loss effects of particles traversing the nuclear medium, are the nuclear modification factor $R_{pPb}$ and the forward-backward asymmetry $R_{FB}$,

$$R_{pPb} = \frac{1}{A_{Pb}} \frac{\sigma_{pPb}}{\sigma_{pp}} \quad \text{and} \quad R_{FB}(|y|) = \frac{\sigma_{pPb}(+|y|)}{\sigma_{pPb}(-|y|)} . \tag{1}$$

The nuclear modification factor measures by how much the $p$-Pb cross-section deviates from the trivial case that the Pb nucleus is a dilute system of independent free nucleons. Although conceptually simple, its determination requires knowledge of the $pp$ cross-section at the nucleon-nucleon centre-of-mass energy of the proton-lead collision, which in absence of direct measurement needs to be estimated by inter- or extrapolation [13, 20, 21]. The forward-backward asymmetry probes nuclear effects by comparing particle production in the hemispheres corresponding to the direction of the proton and that of the nucleus. No reference cross-section is required, but the variable is not sensitive to overall factors in the production cross-sections.

Figure 3 shows results for the nuclear modification factors of $J/\psi$ and $\psi(2S)$ production [11], both for prompt production and for secondary production from $b$-hadron decays. For prompt $J/\psi$ mesons the data are in good agreement with predictions based on leading-order nuclear PDFs. The agreement degrades when using next-to-leading order predictions, but improves again if energy loss effects in the nuclear medium are accounted for. Although the theoretical uncertainties are large, it seems that an overall satisfactory description of the data is feasible when the known effects are taken into account.
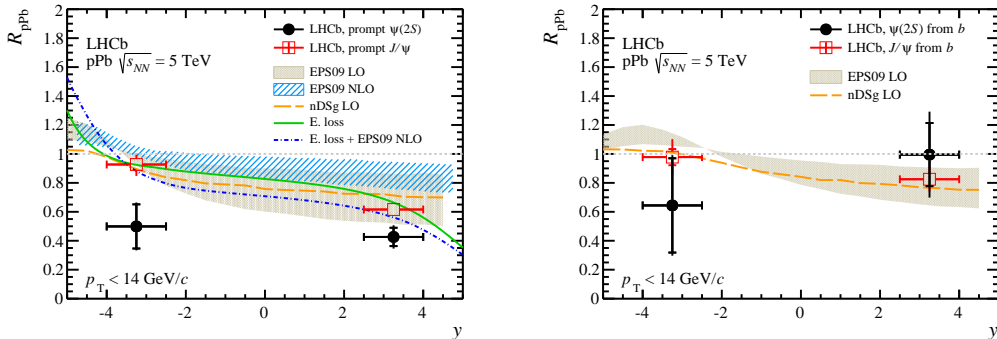


**Figure 3.** Nuclear modification factors for $J/\psi$ and $\psi(2S)$ mesons measured in $p$-Pb collisions by LHCb, (left) for prompt production and (right) for charmonia from $b$-hadron decays, compared to theoretical predictions [15–18].
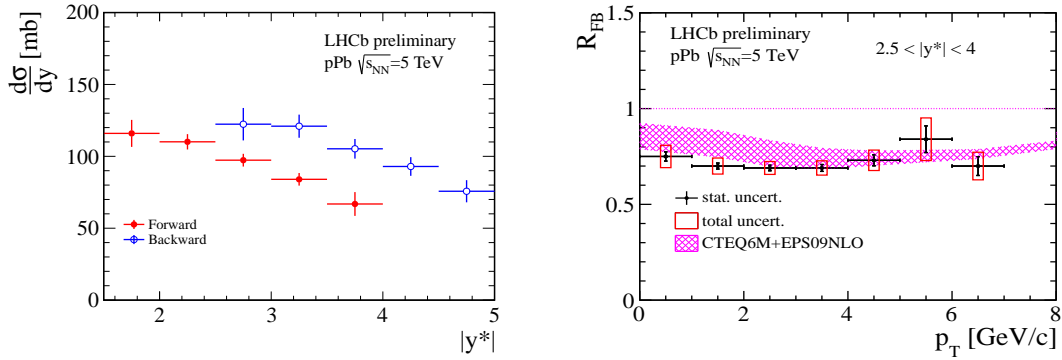
**Figure 4.** $D^0$ production in $p$-Pb collisions, (left) differential cross-section as a function of the absolute value of the rapidity in the nucleon-nucleon centre-of-mass system, and (right) forward-backward asymmetry, calculated from the same absolute rapidity ranges, as a function of the transverse momentum. Due to a boost of 0.47 units in rapidity between lab- and centre-of-mass system, more forward measurements are possible in the direction of the Pb nucleus.
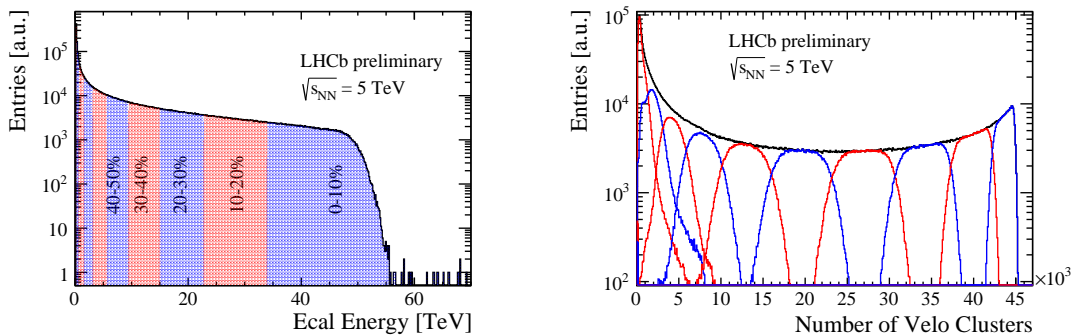


**Figure 5.** (left) ECAL energy deposit of minimum bias Pb-Pb collisions and (right) distributions of the number of VELO clusters for the 10%-quantiles of ECAL energy deposit. For the most central collisions (0-10% quantile) the number of clusters goes into saturation at $45 \times 10^3$.

The nuclear modification factors for prompt $\psi(2S)$ production, especially in the backward region, show larger deviations from unity than for the $J/\psi$, i.e. the data support the picture that the less strongly bound systems are stronger affected by cold nuclear matter effects. For charmonium states from $b$-hadron decays, the nuclear effects are only seen by the $b$-hadron. As a consequence of the tighter binding, nuclear modification factors closer to unity are expected. This is confirmed for the $J/\psi$ from $b$; for the $\psi(2S)$ from $b$ the experimental uncertainties are still to too large for any conclusions. The data are, however, consistent with the expectation that $J/\psi$ and $\psi(2S)$ from $b$-hadron decays are affected in the same way.

Since the products of a breakup of a charmonium state most likely will recombine to open charm mesons, charmonia and open charm mesons are affected differently by the transport properties of the nuclear medium. Additional information is therefore gained from the study of $D^0$ production in $p$-Pb collisions [13], which because of the small charmonium to open charm ratio will not be measurably affected by contributions from charmonium break-up. Figure 4 shows a pronounced forward-backward asymmetry as a function of rapidity in the nucleon-nucleon centre-of-mass system. At the same absolute rapidity, the differential cross-section in the Pb-direction is significantly larger than in the proton direction. The forward-backward asymmetry as a function of transverse momentum is almost constant, in agreement with theoretical expectations. It is, however, worth noting that at small transverse momenta the theoretical uncertainties are much larger than the experimental ones.
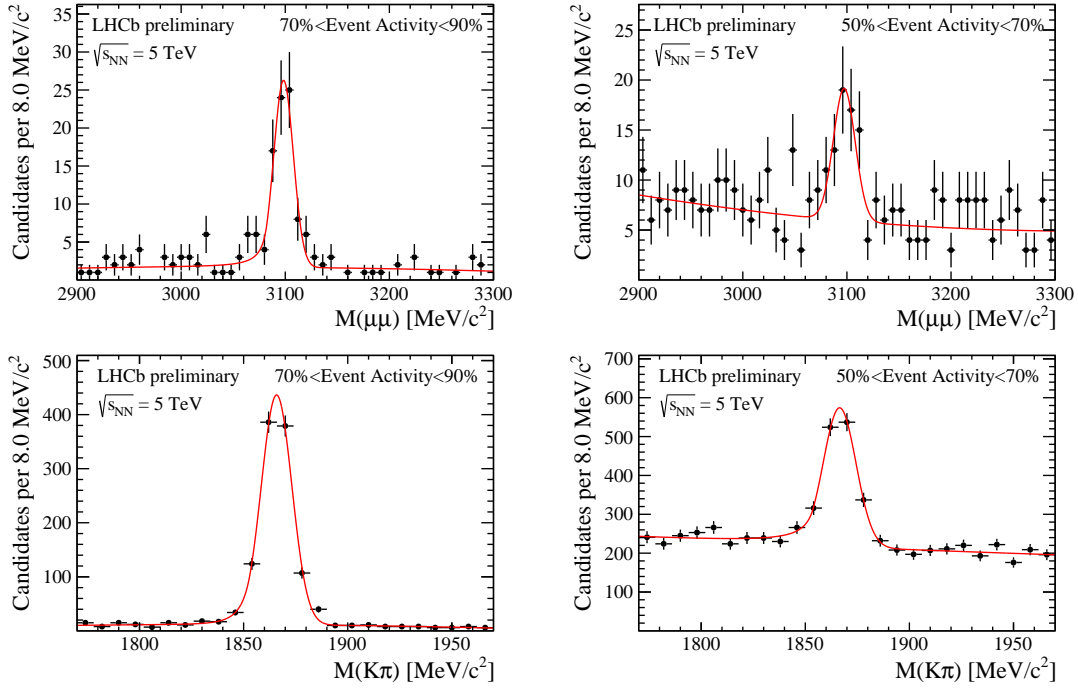
**Figure 6.** Production of (top) $J/\psi$ and (bottom) $D^0$ mesons in (left) peripheral and (right) semi-central Pb-Pb collisions.
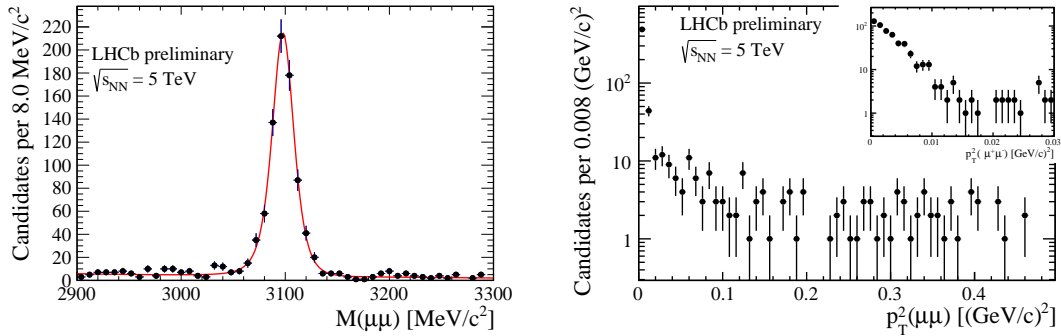


**Figure 7.** $J/\psi$ photoproduction in Pb-Pb collisions, (left) di-muon invariant mass spectrum and (right) transverse momentum distribution. The inset is a zoom of the low-$p_T$ part.

## 4. Lead-lead collisions

Depending on the centrality of the collision, Pb-Pb interactions at the LHC can produce extremely high multiplicity events with correspondingly large energy deposits in the detectors. Figure 5 shows the distribution of the ECAL energy deposit and the distribution of the number of clusters in the VELO. The number of VELO clusters saturates around $45 \times 10^3$. Since the standard pattern recognition program works up to $\sim 30\%$ occupancy in the tracking detectors, physics studies appear feasible up to event activities in the range of the 60–50% quantile of the ECAL energy distribution, *i.e.* for peripheral to semi-central collisions.

Figure 6 illustrates the physics reach of LHCb for Pb-Pb collisions. Clear signals for $J/\psi$ and $D^0$ production are observed in the event activity ranges from 90-70% and from 70-50%, but one also observes a sizeable increase on the background level with higher event activities.

A promising field of study for LHCb are also ultra-peripheral Pb-Pb collisions. An example is shown

in Fig. 7 which shows a $J/\psi$ signal in events where only two muons are recorded in the detector. A very clean signal is observed, with the very soft, exponentially falling $p_T$ spectrum characteristic of coherent photoproduction processes.

## 5. Fixed target physics

Since 2015 fixed target data taking is an integral part of the LHCb ion physics program, which takes advantage of the SMOG system to inject noble gases into the interaction region. Typical gas pressures are of $O(10^{-7})$ mbar, which is sufficient to obtain sizeable samples of beam-gas interaction. Data samples have been recorded with proton or Pb beams on He, Ne and Ar gas. To illustrate the physics prospects, Fig. 8 shows first $J/\psi$ and $D^0$ signals from the study of p-Ne collisions.
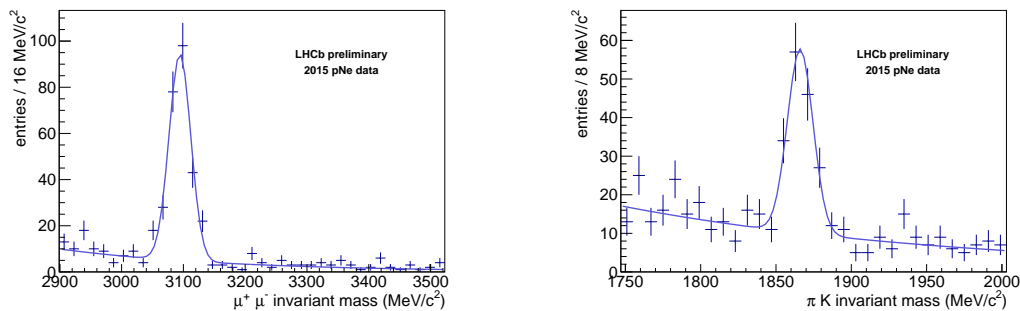


**Figure 8.** Production of (left) $J/\psi$ and (right) $D^0$ mesons in fixed-target p-Ne collisions.

## 6. Summary

In 2013 the LHCb experiment successfully participated in the LHC proton-ion running. Two years later the ion physics program of the experiment was expanded to cover also Pb-Pb collisions and, taking advantage of the SMOG system that allows to inject gas into the LHCb interaction region, the study of fixed target interactions at the LHC. First studies of Pb-Pb collision show that LHCb is able to analyse peripheral to semi-central Pb-Pb collisions.

## References

[1] Matsui T and Satz H 1986 *Phys.Lett.* **B178** 416
[2] Eskola K, Paukkunen H and Salgado C 2009 *JHEP* **04** 065
[3] Arleo F and Peigné S 2012 *Phys.Rev.Lett.* **109** 122301
[4] Alves Jr A A *et al.* (LHCb collaboration) 2008 *JINST* **3** S08005
[5] Aaij R *et al.* (LHCb collaboration) 2015 *Int. J. Mod. Phys.* **A30** 1530022
[6] Barschel C 2014 PhD thesis, RWTH Aachen
[7] Aaij R *et al.* (LHCb collaboration) 2014 *JINST* **9** P12005
[8] LHCb collaboration 2013 LHCb-CONF-2012-034
[9] Aaij R *et al.* (LHCb collaboration) 2014 *JHEP* **02** 072
[10] Aaij R *et al.* (LHCb collaboration) 2014 *JHEP* **07** 094
[11] Aaij R *et al.* (LHCb collaboration) 2016 *JHEP* **03** 133
[12] Aaij R *et al.* (LHCb collaboration) 2014 *JHEP* **09** 030
[13] LHCb collaboration 2016 LHCb-CONF-2016-003
[14] Aaij R *et al.* (LHCb collaboration) 2016 *Phys. Lett.* **B762** 473
[15] Ferreiro E G, Fleuret F, Lansberg J P and Rakotozafindrabe A 2013 *Phys.Rev.* **C88** 047901
[16] Arleo F and Peigné S 2013 *JHEP* **03** 122
[17] Albacete J, Armesto N, Baier R, Barnafoldi G G, Barrette J *et al.* 2013 *Int. J. Mod. Phys.* **E22** 1330007
[18] Conesa del Valle Z, Ferreiro E G, Fleuret F, Lansberg J P and Rakotozafindrabe A 2014 *Nucl.Phys.* **A926** 236
[19] Pivk M and Le Diberder F R 2005 *Nucl.Instrum.Meth.* **A555** 356–369
[20] ALICE and LHCb collaborations 2013 LHCb-CONF-2013-013 & ALICE-PUBLIC-2013-002
[21] ALICE and LHCb collaborations 2014 LHCb-CONF-2014-003 & ALICE-PUBLIC-2014-002